Research Article

Received: 16 June 2018 Revised: 2 October 2018 Accepted article published: 16 November 2018 Published online in Wiley Online Library: 30 December 2018

(wileyonlinelibrary.com) DOI 10.1002/jsfa.9494

Comparison of dynamic water distribution and microstructure formation of shiitake mushrooms during hot air and far infrared radiation drying by low-field nuclear magnetic resonance and scanning electron microscopy

Yuanyuan Zhao,[a] Jinfeng Bi,[a*] Jianyong Yi,[a*] Daniel M Njoroge,[b] Jian Peng[a] and Chunhui Hou[a,c]

Abstract

BACKGROUND: An abundance of shiitake mushrooms is consumed in dried form around the world. In the present study, changes in water state, water distribution and microstructure of shiitake mushrooms during hot-air drying (HAD) and far-infrared radiation drying (FIRD) processes were investigated using low-field nuclear magnetic resonance and scanning electron microscopy. Quality attributes of the dried products were compared in terms of drying property, appearance, rehydration behavior, texture and storage stability.

RESULTS: Compared with HAD, the rate of water diffusion and evaporation of the shiitake mushrooms dried by FIRD was higher, thus resulting in a shorter drying time (630 min), a lower water content (0.07 g g^{-1} wet basis) and a higher glass transition temperature (7.88 °C) for dried products. Moreover, a homogenous and porous microstructure with less shrinkage and case hardening was demonstrated by the FIRD samples, indicating a superior texture, including a larger pileus diameter (3.4 cm), a higher rehydration ratio (7.31), a lower hardness (37.93 N) and a higher crispness (1.41 mm) for FIRD shiitake mushrooms.

CONCLUSION: High-quality shiitake mushrooms with a desirable texture could be produced by FIRD by enhancing the diffusion of internal water and alleviating the case hardening during a relatively short drying process.

Keywords: shiitake mushroom; FIRD; LF-NMR; SEM; water dynamics; case hardening

INTRODUCTION

Shiitake mushrooms (*Lentinula edodes*) comprise the most widely planted and consumed fungi throughout the world, contributing to approximately 40% of worldwide production.[1] Unfortunately, fresh shiitake mushrooms are perishable at room temperature as a result of a high water content [approximately 0.90 g g^{-1} wet basis (wb)] and absent surface cuticle, which are unlikely to protect materials from water loss and physical attack.[2] Hence, a large portion of shiitake mushrooms are treated by various processing procedures.

Drying is one of the most common and effective processing methods for fruit and vegetables, removing water to normally less than 10%. In recent years, a variety of drying methods have been studied with respect to shiitake mushrooms, including hot-air drying,[3] microwave drying,[4] freeze drying[5] and infrared radiation drying.[6] Among these methods, infrared technology was shown to be practical because of its versatility and low capital cost.[7] Krishnamurthy *et al.*[8] found that far-infrared radiation drying (FIRD) is more suitable for food processing because most food materials absorb radiative energy in the far-infrared region (wavelength range 0.75–100 mm). Moreover, some studies have investigated the drying properties of shiitake mushrooms during FIRD and reported that the advantages of FIRD include a high drying rate, energy-saving and the uniform distribution of heat.[9,10]

Moisture diffusion is recognized as one of the main factor affecting drying efficiency.[11] Recently, low-field nuclear magnetic resonance (LF-NMR) has gained popularity as a non-destructive

* *Correspondence to: J Bi or J Yi, Institute of Food Science and Technology, Chinese Academy of Agricultural Sciences, Yuanmingyuan West Road No.2, Haidian District, Beijing 100193, China. E-mail: bjfcaas@126.com (Bi); E-mail: yijianyong515@caas.cn (Yi)*

a *Institute of Food Science and Technology, Chinese Academy of Agricultural Science (CAAS)/Key Laboratory of Agro-Products Processing, Ministry of Agriculture and Rural Affairs, Beijing, China*

b *Institute of Food Bioresources Technology, Dedan Kimathi University of Technology, Nyeri, Kenya*

c *Tianjin University of Science and Technology College of Food Engineering and Biotechnology, Tianjin, China*

and fast technology for measuring water content, state and distribution in fruit and vegetables,[12] including strawberry,[13] cherry tomatoes[14] and broccoli.[15] According to reports by Tian *et al.*[16] and Xu *et al.*,[17] the heat efficiency of infrared radiator construction is possibly associated with the formation of a porous microstructure during the drying process, which further markedly affects the texture of dried products. This is in agreement with other studies that focused on texture quality, including the hardness and rehydration ratios of shiitake mushrooms induced by different drying methods.[3,18] However, the effects of drying on shiitake mushrooms in terms of dynamic changes in water distribution and microstructure modification during the drying process have not been fully clarified. This may restrict the understanding of the texture evolution of shiitake mushrooms during drying, as well as the further selection of a suitable drying technology. Therefore, the present study aimed to explore a preferable drying method between hot-air drying (HAD) and FIRD, with the purpose of improving the drying rate, appearance, hardness and rehydration ability of dried shiitake mushrooms by monitoring the water distribution and microstructure formation via NMR and SEM throughout the whole drying process.

MATERIALS AND METHODS

Materials

Fresh shiitake mushrooms with a mean ± SD diameter of 6.0 ± 0.1 cm were purchased from a local market (Beijing, China). Prior to the experiments, the stalks of the shiitake mushrooms were removed partially. Then, the samples were washed with tap water, dripped and put into plastic bags at 4 °C to achieve an internal moisture equilibrium. The average initial water content of the fresh mushrooms was 11.90 ± 0.13 g g^{-1} db, which was determined after being dried in an oven at 105 °C for 48 h.[19]

Drying methods

Approximately 50.0 ± 1.0 g of fresh shiitake mushrooms were weighed and spread on a wire mesh tray in a single layer in the HAD and FIRD operations. HAD was performed in an electric thermostatic drying oven (DHA-9123A; Jinghong Experiment Instrument Co., Ltd, Shanghai, China). FIRD was carried out in a radiation dryer (700-3; Rongfeng Science Instrument Co., Ltd, Shanghai, China), which consisted of two quartz infrared generators with a radiation range of 5.8–6.2 μm. The radiation distance between oven plate and infrared lamps was 12 cm, and the drying power was 1350 W, in accordance with the optimized parameters reported by Darvishi *et al.*[9] With the purpose of eliminating any difference in drying conditions, the drying temperature and blower speed of both HAD and FIRD were 60 °C and 2 m s^{-1}, respectively.[10] The drying processes was stopped when moisture content of samples achieved approximately 0.11 g g^{-1} db.

Drying properties

The drying curves of the shiitake mushrooms were obtained according to Seremet *et al.*[20] with minor modifications. During the HAD and FIRD drying processes, the shiitake mushrooms were weighed and the moisture content dry basis (db) was calculated according to Eqn (1):

$$M_t = \frac{m_t - m_d}{m_d} \quad (1)$$

where M_t (g g^{-1} db) is the moisture contents at t min, m_t is the dry mass (g) of shiitake mushrooms at t min, and m_d is the final dry mass (g) after drying treatment.

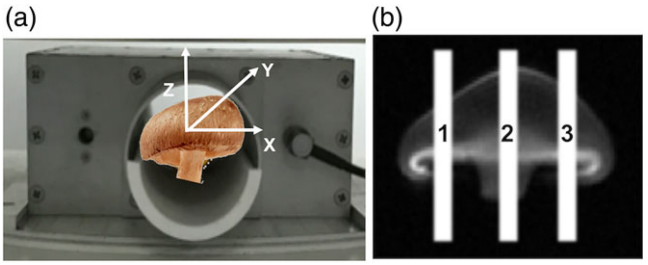

Figure 1. The operation of NMR and MRI on shiitake mushrooms during the HAD and FIRD processes. (a) The chamber of analyzed sample in the LF-NMR machine. (b) The imaging part of the examined shiitake mushrooms.

According to Eqn (1), moisture ratio (MR) and drying rate (DR) were calculated by Eqns (2) and (3), respectively:

$$MR = \frac{M_t - M_e}{M_o - M_e} \quad (2)$$

$$DR = \frac{M_t - M_{t+\Delta t}}{\Delta t} \quad (3)$$

where M_o (g g^{-1} dry basis db) is the initial mass of fresh shiitake mushrooms before drying treatment, M_e (g g^{-1} db) is the final equilibrium moisture content after drying treatment. M_t and $M_{t+\Delta t}$ are the moisture content (g g^{-1} db) at t and $t + \Delta t$, respectively.

Transverse relaxation time (T_2) and magnetic resonance imaging (MRI)

T_2 is one of the proton relaxation parameters because the water fractions have different hydrogen proton activity in different microenvironments and exhibit different T_2 relaxation properties.[21,22] T_2 of three water states (free water, immobilized water and bound water) of shiitake mushrooms during HAD and FIRD processes were determined using a LF-NMR analyzer (MiniMR-60; Niumag Lo. Ltd, Shanghai, China). A 60-mm diameter radio frequency coil was used to collect Carr-Pur-Meiboom-Gill sequence decay signals.[23] A diagram depicting the sample chamber of the NMR machine is provided in Fig. 1(a) and the whole piece of the shiitake mushroom was arranged horizontally on a groove of the cylindrical plastic tube. T_2 analysis was conducted with the following parameters: 90° pulse time = 12 μs, 180° pulse time = 27 μs, sampling points = 640 138, spectral width = 200 kHz, echo count = 16 000, repeat scan frequency = 16, sampling repetition time = 3000 ms. Then, T_2 distribution curves were constructed based on logarithmic coordinates of the original data obtained.

MRI not only effectively characterizes the spatial distribution of the proton signal,[12] but also permits the quantification of water concentration and water mobility in the some specified region.[24] MRI images of the samples were acquired by the same NMR analyzer with MRI, version1.06 (Niumag Lo. Ltd, Suzhou, China). Shiitake mushroom in a vertical direction is shown in Fig. 1(b). The imaging region (scanning slices) of the material during the HAD and FIRD processes was divided into three layers inside the sample, and the scanning slices gap was set from 5.0 to 0.5 mm during the drying processes. Finally, layer 1 (peripheral part) and layer 2 (center part) were captured. MRI was established using the parameters: waiting time = 800 ms, echo time = 13.5 ms, phase size = 192, slices width = 5 mm, sight echography = 80 mm. Measurement of T_2 and MRI was repeated twice.

Microstructure

The microstructures of the shiitake mushroom during the HAD and FIRD processes were investigated using a scanning electron microscope (S-570; Hitachi Co., Ltd, Tokyo, Japan) at an accelerating voltage of 1.0 kV. The samples were carefully cut into cubes with a razor blade. According to Lombraña, Rodríguez and Ruiz,[4] and with some modification, the cubes were fixed, dehydrated stepwise and then dried with a CO_2 tipping point dryer (CPD-020; Balzers Union Co., Ltd, Balzers, Liechtenstein). A manual cross-sectional of the samples was acquired by breaking these cubes from the middle and fixed on the scanning stub. Finally, the samples were sputter-coated with a gold target using an ion sputtering apparatus (MCI000; Hitachi Co., Ltd) and subsequently viewed at magnifications of 100× and 250×, respectively.

Appearance

Images were collected using a DigiEye system (V270; HunterLab, Reston, VA, USA). As reported by Gao *et al.*,[25] the difference in color (ΔE) between the dried mushrooms and fresh materials is given in Eqn (4):

$$\Delta E = \sqrt{\left(\mathrm{L} - L_0\right)^2 + \left(\ a - a_0\right)^2 + \left(\ b - b_0\right)^2} \tag{4}$$

where L, a and b are the lightness, green–red and yellow–blue value of dried shiitake mushrooms, respectively, whereas L_0, a_0 and b_0 are those of the respective fresh samples.

Rehydration ratio (RR)

The RR of the shiitake mushroom dried by HAD and FIRD was measured as described by Giri and Prasad[1] with a few modifications. The dried samples were immersed in distilled water at 40 °C and the ratio of dried mushroom to water was set to 1:10 (w/w). The rehydrated samples were taken out from water bath every 10 min and drained for 30 s on a plate at room temperature, and then they were weighed on an electronic balance. Once the samples reached the constant weight (given to two decimal places), the rehydration process was stopped. RR was calculated using Eqn (5):

$$RR = \frac{M_f}{M_g} \tag{5}$$

where M_f (g) and M_g (g) are the weights of the rehydrated and dried samples, respectively.

Texture

Texture properties (i.e. hardness and crispness) of the final dried products were measured using a texture analyzer with a ball probe (P/0.25 S) (TA. XT 2i/50; Stable Micro System Co., Ltd, Godalming, UK). The penetration distance was 10.0 mm and the compression speeds were 5.0 and 10.0 mm s^{-1} before and after the test, respectively. Hardness and crispness were derived from the force-deformation curve. Texture measurements were conducted in ten pieces of the samples with a similar shape and size.

Water activity (*Aw*) and glass transition temperature (*Tg*)

The dried shiitake mushrooms that were subjected to HAD and FIRD were crushed using a grind machine for a 15-s crush and 20-s rest, repeating this three times to obtain powders, followed by measurement of their *Aw* and *Tg*. *Aw* was determined using an aqualon water activity meter (Decagon, Co., Ltd, Washington, DC, USA). *Tg* was measured through a differential scanning calorimetric (DSC) (Q200, TA Instruments Ltd, Milford, MA, USA). Approximately 10–15 mg of the dried powders was encapsulated in a 50-μL hermetic aluminium pan and sealed. The DSC curve was obtained by cooling the samples to −70 °C and then heating at a rate of 5 °C min^{-1}, up to 100 °C, after an isothermal holding of 2 min. Each thermogram was analyzed to obtain the onset, middle and end of transition, as well as enthalpy of melting, and the middle value of the transition temperature was recorded.

Statistical analysis

All of the measurements were performed in triplicate, unless otherwise specified, and the results were expressed as the average values. Pearson correlation analysis was conducted using Origin, version 8.5 (OriginLab Corp., Northampton, MA, USA). Statistical analysis was carried using SPSS, version 18.0 (SPSS Inc., Chicago, IL, USA). $P < 0.05$ (one-way analysis of variance and Duncan's test) was considered statistically significant with respect to differences among the product quality attributes.

RESULTS AND DISCUSSION

Drying properties

The changes in moisture ratio (MR) and drying rate (DR) of the shiitake mushrooms during the HAD and FIRD processes are depicted in Fig. 2. As shown in Fig. 2(a), the MR of the shiitake mushrooms was decreased significantly with an extension of drying time for both processes. The drying time of the shiitake mushrooms treated by FIRD process was 630 min, which was reduced by 22.2% compared to that of the HAD process (810 min). Correspondingly, as shown in Fig. 2(b), the DR of the FIRD shiitake mushrooms was higher than that of the samples dried by HAD during the initial and final stages of the drying process. The initial DR of the shiitake mushrooms during FIRD process (0.056 g g min^{-1}) was significantly higher ($P < 0.05$) than that of the HAD samples (0.024 g g min^{-1}), indicating the superior thermal property of FIRD. This was in agreement with the results of studies by Salehi *et al.*[10] and Deng *et al.*[26] who found that the heat efficiency of infrared radiator construction is approximately 80%, leading to a higher rate of water removal compared to HAD. However, the DR gradually decreased with a continuous decrease of water content during both drying processes, implying a reduced rate of moisture diffusion. This may possibly be attributed to the low content of free water and tissue shrinkage of the shiitake mushrooms in the final drying stage. Thus, changes in water states and microstructure are further characterized below.

Fitting curve of the signal amplitude and moisture content

The correlation between total signal amplitude (TSA) of magnetic resonance from NMR analysis and the moisture content of the shiitake mushrooms is shown in Fig. 3. Liner relationships between TSA and moisture content of the HAD and FIRD dried samples were found with corresponding correlation coefficients of 0.9418 and 0.9859, respectively. These results coincide with those of the study by Lv *et al.*[27] who reported significant positive correlations between TSA and moisture content for six different vegetables treated by microwave vacuum drying. Therefore, it was suggested that LF-NMR could be applied to predict the water dynamics of shiitake mushrooms during drying processes.

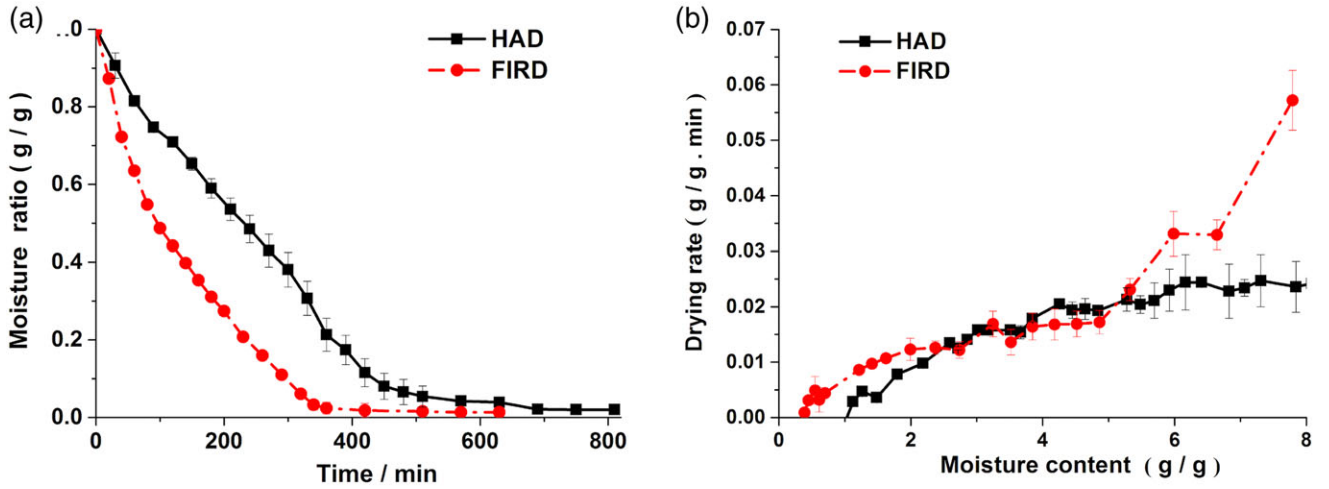

Figure 2. The drying kinetics of shiitake mushrooms during the HAD and FIRD processes. (a) The moisture ratios of the shiitake mushrooms during the drying processes. (b) The drying rates of the shiitake mushrooms during the drying processes. Bars represent the mean ± SD ($n = 3$).

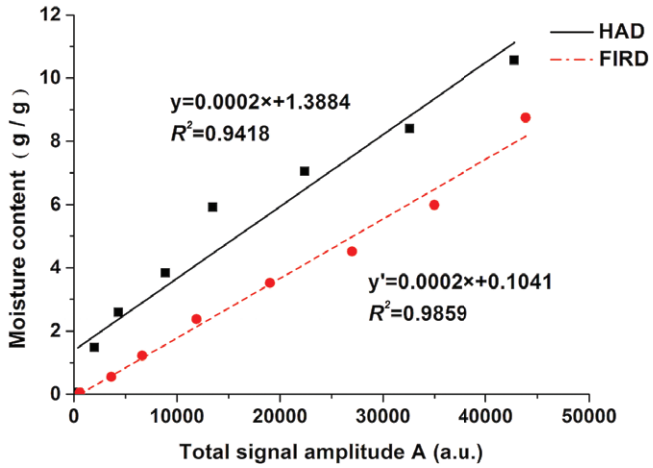

Figure 3. The correlation between the total signal amplitude and the moisture content of shitake mushrooms during the drying process. The correlation was performed by using Pearson correlation analysis in Origin.

T_2 inversion spectra curves

T_2 denotes a higher binding energy and mobility of the water components: bound water at 0.01–10 ms (T_{21}), immobilized water at 10–100 ms (T_{22}) and free water at 100–1000 ms (T_{23}).[28] The amounts of the three water states were observed from peak areas (A_2), and the corresponding peak areas are marked as A_{21}, A_{22} and A_{23}.[12] As shown in Fig. 4(a, b), a drastic decrease of A_{23} and a slight decrease of A_{22} was observed with a decrease in total moisture content during the initial drying process. Meanwhile, the T_{22} and T_{23} of the samples were marginally reduced, which showed that curves were shifted to the lower relaxation direction. Generally, the decrease of A_2 and T_2 not only demonstrated the constant water evaporation during drying, but also confirmed that the mobility of free water and immobilized water gradually declined. Jin *et al.*[15] and Li *et al.*[26] also found that water mobility was highly related to the drying method. Song *et al.*[29] further reported that reduced T_{22} and T_{23} were related to the breakdown of microstructure. In the subsequent drying process, the residual amount of immobilized water (A_{22}) was higher than that of free water (A_{21}), which signified that immobilized water became the main water state of the shiitake mushrooms at a certain time and was relatively difficult to remove. Finally, as shown in Fig. 4(c), bound water appeared in the HAD and FIRD samples after drying for 450 min, reflecting the bound water being tightly combined with mushroom hyphae.

Moreover, as shown in Fig. 4(a, b), the decrease of A_{22} and A_{23} in FIRD samples was obviously quicker than that in HAD samples during the whole drying processes. In addition, the immobilized water became the main water state in the FIRD samples after being dried for 180 min (Fig. 4b), whereas this change occurred in the HAD samples at 450 min. Moreover, the A_2 of the three water state of FIRD samples was clearly lower than that of the HAD samples at 810 min (Fig. 4d), demonstrating a lower water content of the final FIRD products. Correspondingly, as shown in Table 1, the water content of final shiitake mushroom dried by FIRD was 0.07 g g^{-1} wb, which was lower than that of the HAD samples (0.11 g g^{-1} wb). Furthermore, the A_{22} of the FIRD samples was lower than that of the HAD samples (Fig. 4d), showing a lower content of immobilized water of the final FIRD products. As reported by Li *et al.*,[30] a certain amount of immobilized water could transform to free water and subsequently diffuse from inside of the material to the outside during the drying process. Accordingly, it could be concluded that FIRD is likely to promote the continuous evaporation of free water and accelerate the transforming behavior of immobilized water into free water.

MRI

The MRI can help visualize the water spatial distribution.[17] As shown in Fig. 5, a higher proton signal density of images was observed in the stalk of the mushroom compared to that of the cap, indicating that water was mainly located in the stalk of fresh shiitake mushroom. With an extension of drying time, red regions disappeared and the size of green regions gradually decreased, which indicated water loss during both drying processes. This phenomenon was in agreement with the findings of Cheng *et al.*[31] who also investigated themoisture distribution during HAD using MRI, and discovered that changes in water distribution were significantly related to the drying process. It worth noting that a higher signal amplitude was detected in the periphery section of the samples examined during the FIRD (Fig. 5c4) than that of the samples during the HAD after drying for 180 min (Fig. 5a4). However, as shown in Fig. 2, the MR of the HAD samples was significantly higher

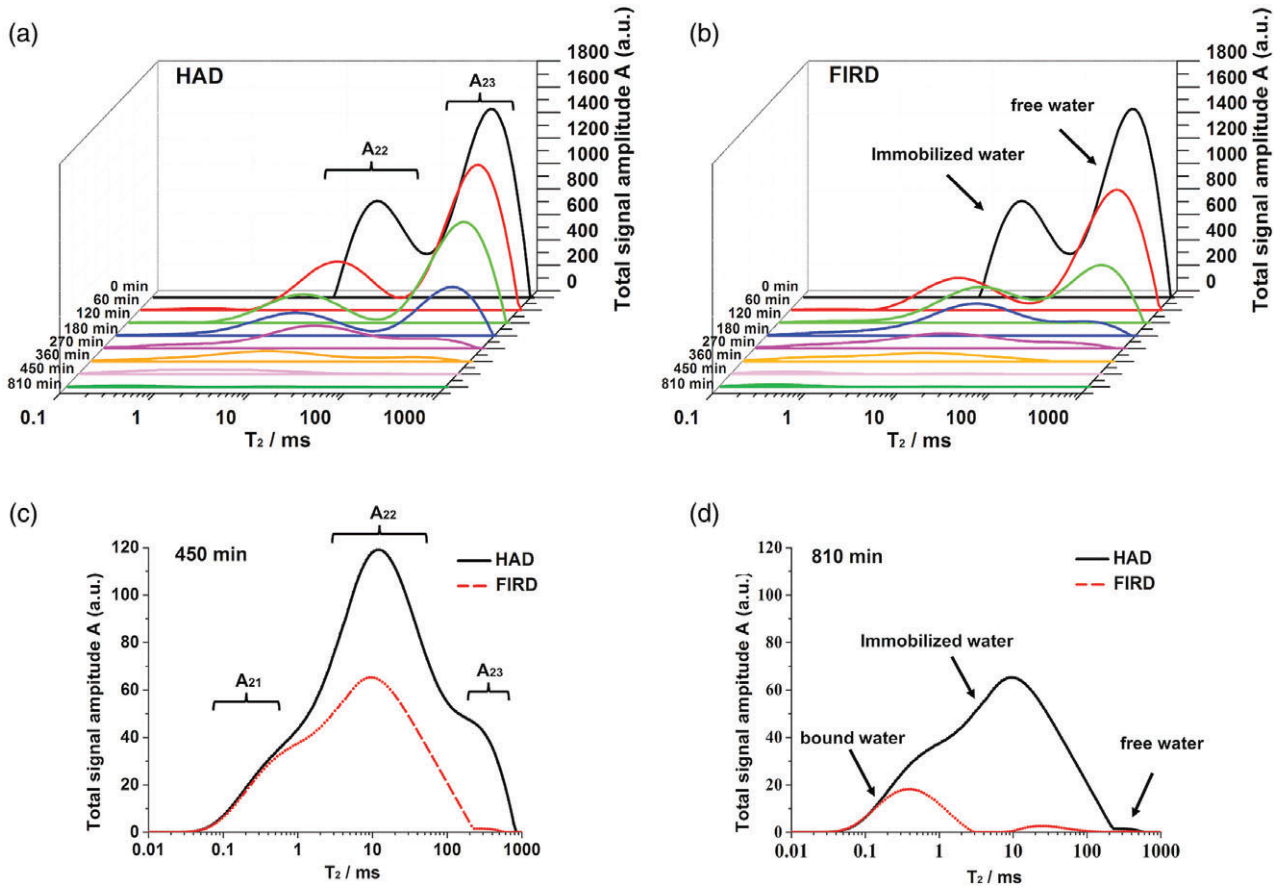

Figure 4. The T_2 inversion spectra curve of shiitake mushrooms at each drying stage during the HAD and FIRD processes. (a, b) T_2 inversion spectra curve of the whole HAD and FIRD processes, respectively. (c, d) T_2 inversion spectra curve of the HAD and FIRD processes at 450 and 810 min, respectively.

Table 1. The physical properties of the final dried shiitake mushrooms dried by the HAD and FIRD methods

	HAD	FIRD
ΔE_c	9.37 ± 0.64^a	6.10 ± 0.52^b
ΔE_g	24.82 ± 0.89^a	15.53 ± 0.11^b
Hardness (N)	123.29 ± 0.16^a	37.93 ± 0.56^b
Crispness (mm)	0.68 ± 0.16^b	1.41 ± 0.59^a
Water content (g g^{-1} wb)	0.11 ± 0.04^a	0.07 ± 0.02^b
Aw	0.35 ± 0.00^a	0.27 ± 0.00^b
Tg (°C)	6.56 ± 0.07^b	7.88 ± 0.27^a
RR	4.64 ± 0.32^b	7.31 ± 0.95^a

Data are expressed as the mean ± SD.
For hardness and crispness, $n = 10$; for other properties, $n = 3$.
Different lowercase letters in the same column indicate a statistical difference at $P < 0.05$.
HAD, hot-air drying; FIRD, far-infrared radiation drying; ΔE_c *and* ΔE_g are the color difference between fresh materials and dried mushroom cap and gill, respectively; *Aw*, water activity; *Tg*, glass transition temperature; RR, rehydration ratio.

($P < 0.05$) than that of the FIRD samples throughout the whole process. This illustrated that FIRD showed a better ability than HAD to improve the constantly rapid water removal from the center to the outside of the mushrooms. Moreover, compared with the FIRD samples (Fig. 5d5), a certain amount of water was locked in edge area of the HAD samples at 270 min (Fig. 5b5), which was characterized by the relatively higher signal density (red region). Thus, this implied that water mobility become slow after being subjected to HAD for 180 min, and water diffusion might be restricted in the later stage, which resulted in the water population collecting in the outside part of HAD samples instead of evaporating. The above-mentioned results confirmed that water diffusion could be continuously accelerated by FIRD, whereas this was restricted and water was harder to transfer towards the outside in the later stage of the HAD process. The superiority of FIRD was mostly attributed to its higher water mobility conmpared to HAD, which could be a result of the strong penetrability and high thermal effect of far-infrared radiation. According to the FIRD principle reported by Krishnamurthy *et al.*,[8] when foods are subjected to far-infrared field, the radiation penetrates directly into the inner materials, and then the vibration of the internal water molecules is quickly promoted, hence reducing the binding force between water molecules and surrounding hyphae. In this case, FIRD may cause constantly rapid water removal from the center to the outside.

Microstructure

The microstructure of shiitake mushrooms dried by HAD and FIRD was captured using SEM. In Fig. 6(a1–d1), numerous waterish hyphae spread over fresh shiitake mushrooms, and an irreversible collapse of microstructure subsequently occurred when shiitake mushrooms were subjected to drying. The shrinkage of porous

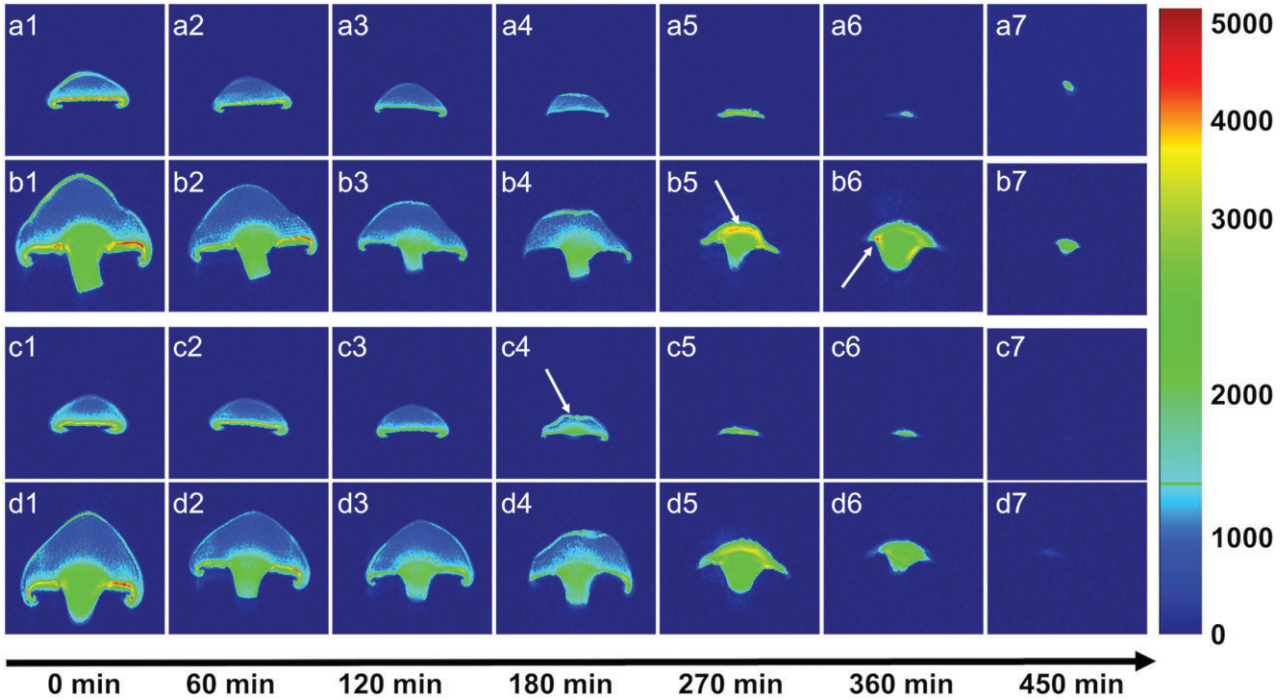

Figure 5. MRI images of shiitake mushrooms at each drying stage during the HAD and FIRD processes. (a1–7, b1–7) Images of part 1 and part 2 of the shiitake mushrooms during HAD drying, respectively. (c1–7, d1–7) Images of the shiitake mushrooms during FIRD drying. Bar on the right indicates the NMR spectral band, and the blue to red of the image color indicates the proton signal density from low to high proton signal density.

material during drying results from a lowering of the liquid pressure induced by the desaturation process at the interface.[32] Furthermoe, the product loses water and then collapses under its own weight because glass transition does not take place during the main phase of drying process.[33] In particular, the microstructure of the mushrooms induced by HAD gradually become tight, as clearly indicated in Fig. 6(a6–a7). The hyphae of the HAD samples were damaged seriously and the shrinkage was obvious, thus creating a compact microstructure with low porosity (Fig. 6b7). Such a microstructure could be ascribed to the relatively poor drying properties of HAD. Samples with a high water content were heated by hot air blowing on the surface and thus the surface temperature of the samples was higher than the inside temperature; however, a higher water content was located in the center of the shiitake mushrooms (Fig. 5b1, d1). In this case, the direction of temperature and humidity gradient of the sample was opposite during the HAD process. Consequently, the rate of water migration from the center to the surface of the samples was slower than that of water evaporation from the surface to the surrounding environment. This phenomenon gave rise to a dense microstructure (Fig. 6b8) with an obvious crust (Fig. 6a8) in the surface of HAD samples. The case hardening of the HAD samples could slow down moisture removal during HAD drying, which might explain why moisture transfer from the center to the surface was restricted. Specifically, the residual amount of the free water (A_{23}) of HAD samples was lower than that of the FIRD samples as shown in Fig. 4(c), and a higher signal amplitude of HAD than FIRD was detected at 450 min. The hindered water evaporation of shiitake mushrooms after being dryed for 450 min could be associated with the compact microstructure, as indicated by case hardening of the shiitake mushrooms treated by HAD (Fig. 6a7, a8), leading to a longer drying time for HAD compared to FIRD (Fig. 2a).

By contrast, a loose and porous microstructure was exhibited by the FIRD mushrooms (Fig. 6c8, d8). FIRD could stimulate water diffusion from the center to the surface of the mushroom and create a uniform water distribution thoughout the whole drying process, thus promoting the formation of a porous microstructure and alleviating case hardening. This good drying property was the result of infrared radiation penetrating directly into the inner materials and generating heat, which motivated the vibration of internal water molecules, consequently inducing the water inside to constantly move outwards.[7,8] In conclusion, the changes in water distribution and microstructure of the shiitake mushrooms could be attributed to the behavior of the drying properties of HAD and FIRD, for which the structure, in turn, could affect further moisture diffusion in the subsequent drying process.

Appearance

Changes in the shape, size and color of the shiitake mushrooms during the HAD and FIRD processes are shown in Fig. 7. Generally, shrinkage is one of the main attributes affecting the quality of dried products as perceived by consumers.[34] The diameter of the fresh mushroom was approximately 6.0 ± 0.1 cm, shrinking to 3.4 ± 0.1 cm and 3.9 ± 0.1 cm after being exposed to HAD and FIRD for 810 min, respectively. Furthermore, the sizes of mushrooms at each stage of the FIRD process were bigger than that of HAD samples at the same stage. Thus, a bigger volume and less shrinkage of shiitake mushrooms were obtained by FIRD compared to HAD. Indeed, different degrees of shrinkage of macroscopic mushroom were generated when water migrated from the center towards surface during drying, which was reflected as a change in shape.[33] Nowak and Lewicki[35] also reported that higher outward moisture flux during FIRD process could be one of the main reasons why shrinkage of materials is prevented.

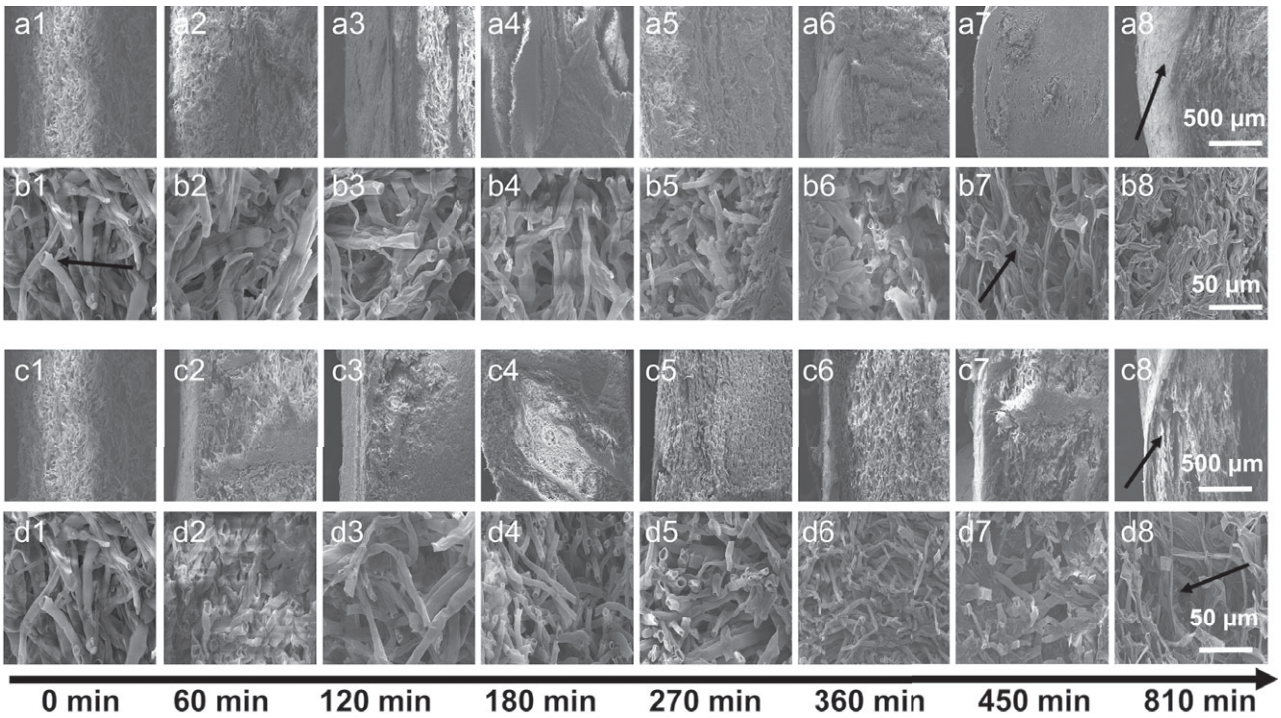

Figure 6. The microstructure changes of shiitake mushrooms at each drying stage during the HAD and FIRD processes made using a scanning electronic microscope. (a1-8, b1-8) Images of the HAD dried samples captured in magnification at 100× and 250×, respectively. (c1-8, d1-8) Images of the shiitake mushrooms during FIRD drying.

Figure 7. The appearance of the whole dried shiitake mushroom at each drying stage of the HAD and FIRD processes.

Color is considered as another important quality-related parameter of dried mushrooms. Figure 7 demonstrates a decrease in lightness of all of the shiitake mushrooms during drying. The darken appearance was a result of melanins, as produced by non-enzymatic browning, such as the Maillard reaction.[36] Because of the higher water content of dried shiitake mushrooms, the Maillard reaction was easily triggered in HAD samples compared to FIRD samples. Correspondingly, as shown in Table 1, the ΔE values of the cap and gill of whole pieces of FIRD dried samples were 6.10 ± 0.52 and 15.53 ± 0.11, which were significantly lower ($P < 0.05$) than those of the HAD dried samples (9.37 ± 0.64 and 24.82 ± 0.89, respectively). Therefore, a relatively lower degree of browning was demonstrated in the FIRD process.

Rehydration properties

Rehydration characteristics of final products dried by HAD and FIRD after rehydration for 2 h are shown in Fig. 8. In Fig. 8(a), the RR of the FIRD dried samples was significantly higher ($P < 0.05$) than that of the HAD dried samples during the whole rehydration process. Furthermore, the final RR of the FIRD dried samples after 200 min reached 7.31 ± 1.72. Moreover, with regard to the T_2 inversion spectra curve in Fig. 8(b), a higher TSA was observed in the FIRD shiitake mushrooms, indicating a higher water absorption compared to that of the HAD samples. Interestingly, A_{22} was bigger than A_{23} in both rehydrated mushrooms, which could imply that immobilized water was the predominant state of water in the rehydrated mushrooms. Nevertheless, more effort should be made to clarify the changes in water state of shiitake mushrooms during the rehydration process. Additionally, as shown in Fig. 8(c), a large amount of water was distributed in the periphery of rehydrated mushrooms, demonstrating that the direction of water absorption was from the outside to the inside. Furthermore, a bigger area of high signal amplitude (red region) was observed in FIRD samples, indicating that water diffusion was relatively easier for the FIRD samples and absorbed much more water than the HAD samples. Furthermore, dried shiitake mushrooms could not return to the original shape of the fresh materials, as shown in Fig. 8(d), which might be a result of microstructural damage (Fig. 6). Some researchers report that the irreversible structural damages are probably a result of reduced rehydrated properties.[37] HAD samples could not restore the smooth surfaces and circle shape, which was attributed to case hardening and relatively serious shrinkage, leading to insufficient absorption. Conversely, FIRD mushrooms clearly recovered to a shape similar to that of fresh samples after rehydration for 200 min, as reflected by a plump and round shape attributed to sufficient water absorption (Fig. 8c, d). This good rehydration ability was the consequence of loose hyphae structure and less shrinkage, as discussed above with respect to the results of microstructure (Fig. 6c8) and appearance (Fig. 7).

Texture, A_w and T_g

The texture (hardness and crispness), *Aw* and *Tg* of the final products dried by HAD and FIRD are shown in Table 1. The hardness of

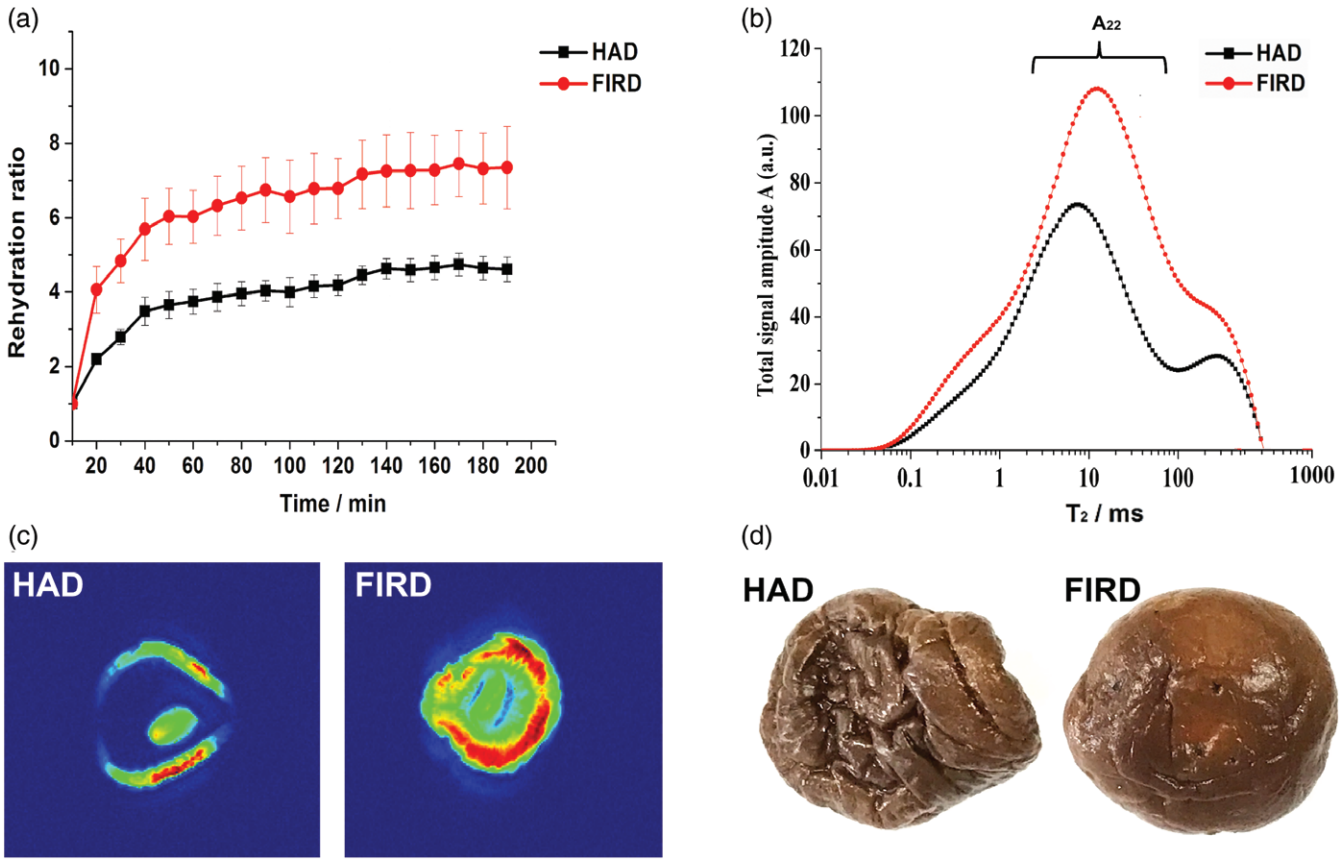

Figure 8. The rehydration properties of the dried shiitake mushroom produced by HAD and FIRD after rehydrating for 200 min. (a) The rehydration ratio curve during rehydration process. Bars represent the mean ± SD ($n = 3$). (b) T_2 inversion spectra curve of the rehydrated samples. (c) MRI images of the rehydrated samples. (d) The appearance of the rehydrated samples. For differences in the color, see Fig. 5.

the FIRD dried shiitake mushrooms was 37.93 ± 0.56 N, which was lower than that of the HAD dried samples (123.29 ± 0.16 N). For crispness, that of FIRD dried samples was 1.41 ± 0.59 mm, which was higher than that of HAD dried samples (0.68 ± 0.16 mm). Generally, hardness, crispness and RR of dried products are the macroscopic manifestation of microstructures. Thus, the better texture of FIRD dried mushrooms was a result of the superior porous structure, as indicated in Fig. 6d8. Additionally, the final moisture content of the FIRD dried samples (0.11 ± 0.04 g g^{-1} db) was lower than that of the HAD dried samples (0.07 ± 0.02 g g^{-1} db) after drying for 810 min (Table 1), which was considered as another reason for the relatively lower hardness. The A_w of the final dried mushrooms subjected FIRD was 0.27, which was lower than that of the HAD samples (0.35). This demonstrated that there was a better stability in FIRD samples, which could inhibit the growth of micro-organisms and reduce rates of chemical reactions during storage.[36] Similarly, *Tg* is related to the storage ability of dried products.[38] The *Tg* of shiitake mushrooms dried by FIRD was 7.88 ± 0.27 °C, which was higher than that of the HAD samples (6.56 ± 0.07 °C). Xu *et al.*[39] reported that FIRD may appreciably enhance *Tg* of the dried carrot with a decrease of water content during drying, especially being affected by an immobilized water content and its decreased mobility. Correspondingly, as seen in Fig. 4(d), the immobilized water content of the FIRD dried samples was lower than that of the HAD dried samples, which was consistent with a higher *Tg* of the FIRD samples. Therefore, the shiitake mushrooms subjected to FIRD have a better storage ability.

CONCLUSIONS

The different effects of the HAD and FIRD processes on the dynamic water distribution and microstructure formation were compared, as well as the correlation between them at different drying times. Compared with HAD, continuous water diffusion and a high rate of water removal were induced by FIRD, which was attributed to its good radiative penetrability and thermal conduction. Meanwhile, the moderate moisture removal rate and uniform water distribution of FIRD could help to create and maintain the porous microstructure of shiitake mushrooms. Notably, FIRD could continuously accelerate water removal to the surface in the later drying stage as a result of less shrinkage, revealing the slow formation rate of the outside crust. Moreover, the alleviative effect of the case hardening phenomenon could enable an improvement in subsequent water removal and allow energy saving and quality improvement. Furthermore, the porous microstructure resulted in good appearance, a better texture and a superior rehydration ability of FIRD shiitake mushrooms. Therefore, FIRD was suggested as a preferable drying technology for the production of high-quality dried shiitake mushrooms.

ACKNOWLEDGEMENTS

This work was supported by the National Key R&D Program of China (2016YFD0400700, 2016YFD0400704) and Collaborative Innovation Task of CAAS (CAAS-XTCX2016005-3-5). The authors declare that they have no conflicts of interest.

REFERENCES

1 Giri SK and Prasad S, Drying kinetics and rehydration characteristics of microwave-vacuum and convective hot-air dried mushrooms. *J Food Eng* **78**:512–521 (2007).
2 Singh P, Langowski HC, Wani AA and Saengerlaub S, Recent advances in extending the shelf life of fresh Agaricus mushrooms: a review. *J Sci Food Agric* **90**:1393–1402 (2010).
3 Kotwaliwale N, Bakane P and Verma A, Changes in textural and optical properties of oyster mushroom during hot air drying. *J Food Eng* **78**:1207–1211 (2007).
4 Lombraña JI, Rodríguez R and Ruiz U, Microwave-drying of sliced mushroom, analysis of temperature control and pressure. *Innovative Food Sci Emerg Technol* **11**:652–660 (2010).
5 Pei F, Shi Y, Mariga AM, Yang WJ, Tang XZ, Zhao LY *et al.*, Comparison of freeze-drying and freeze-drying combined with microwave vacuum drying methods on drying kinetics and rehydration characteristics of button mushroom (*Agaricus bisporus*) slices. *Food Bioprocess Technol* **7**:1629–1639 (2013).
6 Wang HC, Zhang M and Adhikari B, Drying of shiitake mushroom by combining freeze-drying and mid-infrared radiation. *Food Bioprod Process* **94**:507–517 (2015).
7 Doymaz İ, Infrared drying of button mushroom slices. *Food Sci Biotechnol* **23**:723–729 (2014).
8 Krishnamurthy K, Khurana HK, Soojin J, Irudayaraj J and Demirci A, Infrared heating in food processing: an overview. *Compr Rev Food Sci Food Saf* **7**:2–13 (2008).
9 Darvishi H, Najafi G, Hosainpour A, Khodaei J and Aazdbakht M, Far-infrared drying characteristics of mushroom slices. *Chem Prod Process Model* **8**:107–117 (2013).
10 Salehi F, Kashaninejad M and Jafarianlari A, Drying kinetics and characteristics of combined infrared-vacuum drying of button mushroom slices. *Heat Mass Transfer* **53**:1751–1759 (2016).
11 Khir R, Pan Z, Salim A, Hartsough BR and Mohamed S, Moisture diffusivity of rough rice under infrared radiation drying. *LWT – Food Sci Technol* **44**:1126–1132 (2011).
12 Kirtil E and Oztop MH, ^{1}H Nuclear magnetic resonance relaxometry and magnetic resonance imaging and applications in food science and processing. *Food Eng Rev* **8**:1–22 (2015).
13 Otero L and Préstamo G, Effects of pressure processing on strawberry studied by nuclear magnetic resonance. *Innovative Food Sci Emerging Technol* **10**:434–440 (2009).
14 Ciampa A, Dell'Abate MT, Masetti O, Valentini M and Sequi P, Seasonal chemical-physical changes of PGI Pachino cherry tomatoes detected by magnetic resonance imaging (MRI). *Food Chem* **122**:1253–1260 (2010).
15 Jin X, Sman RGMVD, Gerkema E, Vergeldt FJ, As HV and Boxtel AJBV, Moisture distribution in broccoli: measurements by MRI hot air drying experiments. *Procedia Food Sci* **1**:640–646 (2011).
16 Tian Y, Zhao Y, Huang J, Zeng H and Zheng B, Effects of different drying methods on the product quality and volatile compounds of whole shiitake mushrooms. *Food Chem* **197**:714–722 (2016).
17 Xu F, Jin X, Zhang L and Chen XD, Investigation on water status and distribution in broccoli and the effects of drying on water status using NMR and MRI methods. *Food Res Int* **96**:191–197 (2017).
18 García-Segovia P, Andrés-Bello A and Martínez-Monzó J, Rehydration of air-dried shiitake mushroom (*Lentinus edodes*) caps: comparison of conventional and vacuum water immersion processes. *LWT – Food Sci Technol* **44**:480–488 (2011).
19 AOAC, *Official Methods of Analysis*, 15th edn. Association of Official Analytical Chemists, Arlington, VA (1990).
20 Seremet L, Botez E, Nistor OV, Andronoiu DG and Mocanu GD, Effect of different drying methods on moisture ratio and rehydration of pumpkin slices. *Food Chem* **195**:104–109 (2016).
21 Cheigh CI, Wee HW and Chung MS, Caking characteristics and sensory attributes of ramen soup powder evaluated using a low-resolution proton NMR technique. *Food Res Int* **44**:1102–1107 (2011).
22 Lin S, Yang S, Li X, Chen F and Zhang M, Dynamics of water mobility and distribution in soybean antioxidant peptide powders monitored by LF-NMR. *Food Chem* **199**:280–286 (2016).
23 Li T, Rui X, Wang K, Jiang M, Chen X, Li W *et al.*, Study of the dynamic states of water and effects of high-pressure homogenization on water distribution in tofu by using low-field nuclear magnetic resonance. *Innovative Food Sci Emerg Technol* **30**:61–68 (2015).
24 Marcone MF, Wang S, Albabish W, Nie S, Somnarain D and Hill A, Diverse food-based applications of nuclear magnetic resonance (NMR) technology. *Food Res Int* **51**:729–747 (2013).
25 Gao K, Zhou L, Bi J, Yi J, Wu X, Zhou M, *et al.*, Evaluation of browning ratio in an image analysis of apple slices at different stages of instant controlled pressure drop-assisted hot-air drying (AD-DIC). *J Sci Food Agric* **97**:2533–2540 (2017).
26 Deng Y, Wang Y, Yue J, Liu Z, Zheng Y, Qian B, *et al.*, Thermal behavior, microstructure and protein quality of squid fillets dried by far-infrared assisted heat pump drying. *Food Control* **36**:102–110 (2014).
27 Lv W, Zhang M, Bhandari B, Li L and Wang Y, Smart NMR method of measurement of moisture content of vegetables during microwave vacuum drying. *Food Bioprocess Technol* **10**:2251–2260 (2017).
28 Su Y, Zhang M, Fang Z and Zhang W, Analysis of dehydration kinetics, status of water and oil distribution of microwave-assisted vacuum frying potato chips combined with NMR and confocal laser scanning microscopy. *Food Res Int* **101**:188–197 (2017).
29 Song Y, Zang X, Kamal T, Bi J, Cong S, Zhu B *et al.*, Real-time detection of water dynamics in abalone (*Haliotis discus hannai Ino*) during drying and rehydration processes assessed by LF-NMR and MRI. *Drying Technol* **36**:72–83 (2018).
30 Li R, Liu C, Zhang C, Shen J, Wang L and Jia C, Moisture transformation and transport during the drying process for *Radix Paeoniae Alba* slices. *Appl Therm Eng* **110**:25–31 (2017).
31 Cheng S, Zhang T, Yao L, Wang X, Song Y, Wang H *et al.*, Use of low field-NMR and MRI to characterize water mobility and distribution in Pacific oyster (*Crassostrea gigas*) during drying process. *Drying Technol* **36**:630–636 (2018).
32 Kingsly ARP, Meena HR, Jain RK and Singh DB, Shrinkage of ber (*Zizyphus mauritian L.*) fruits during sun drying. *J Food Eng* **79**:6–10 (2007).
33 Madiouli J, Sghaier J, Lecomte D and Sammouda H, Determination of porosity change from shrinkage curves during drying of food material. *Food Bioprod Process* **90**:43–51 (2012).
34 Li J and Qian ZQ, The application of image acquisition and analysis techniques to the field of drying. *Food Eng Rev* **9**:13–35 (2016).
35 Nowak D and Lewicki PP, Quality of infrared dried apple slices. *Drying Technol* **23**:831–846 (2005).
36 Bonazzi C and Dumoulin E, Quality changes in food materials as influenced by drying processes. *Mod Dry Technol* **3**:1–20 (2011).
37 Krokida MK, Tsami E and Maroulis ZB, Kinetics on color changes during drying of some fruits and vegetables. *Drying Technol* **16**:667–685 (1998).
38 Tylewicz U, Aganovic K, Vannini M, Toepfl S, Bortolotti V, Rosa MD *et al.*, Effect of pulsed electric field treatment on water distribution of freeze-dried apple tissue evaluated with DSC and TD-NMR techniques. *Innovative Food Sci Emerg Technol* **37**:352–358 (2016).
39 Xu C, Li Y and Yu H, Effect of far-infrared drying on the water state and glass transition temperature in carrots. *J Food Eng* **136**:42–47 (2014).

